Advanced Filter Design

Miroslav D. Lutovac and Dejan V. Tošić
Dept. of Electrical Engineering
University of Belgrade, P.O. Box 35-54
11120 Belgrade, Yugoslavia
elutovac@ubbg.etf.bg.ac.yu
etosicde@ubbg.etf.bg.ac.yu

Brian L. Evans
Engineering Science Building
Dept. of Electrical and Computer Engineering
The University of Texas at Austin
Austin, TX 78712-1084
bevans@ece.utexas.edu

Abstract

Classical filter design techniques return only one design from an infinite collection of alternative designs, or fail to design filters when solutions exist. These classical techniques hide a wealth of alternative filter designs that are more robust when implemented in analog circuits, digital hardware, and embedded software. In this paper, we present (1) case studies of optimal analog and digital IIR filters that cannot be designed with classical techniques, and (2) the formal, mathematical framework that underlies their solutions. We have automated the advanced filter design techniques in software.

1. Introduction

In designing analog and digital IIR filters, one generally relies on canned software routines or mechanical table-oriented procedures. The primary reason for these "black box" approaches is that the approximation theory that underlies filter design includes complex mathematics. Unfortunately, conventional approaches return only one design, thereby hiding a wealth of alternative filter designs that are more robust when implemented in analog circuits, digital hardware, and embedded software. In addition, conventional approaches may fail to find a filter when in fact one exists.

We develop advanced design techniques to find a comprehensive set of optimal designs to represent the infinite solution space. The optimal designs include filters that have minimal order, minimal quality factors, minimal complexity, minimal sensitivity to pole-zero locations, minimal deviation from a specified group delay, approximate linear phase, and minimized peak overshoot. For digital filters, the design space also includes filters with power-of-two coefficients. We base our approach on formal, mathematical properties of Jacobi elliptic functions [1, 2]. We automate these advanced filter design techniques in software [3, 4].

The key observations underlying advanced filter design are that

1. many designs satisfy the same user specification;
2. Butterworth and Chebyshev IIR Filters are special cases of Elliptic IIR Filters; and
3. minimum-order filters may not be as efficient to implement as some higher-order filters.

We first review our case studies in minimizing quality factors for a switched-capacitor filter design from a finite set of manufactured sections [5] and a reduced multiplier filter [6]. In both cases, the filter optimization problem is a mixed-integer linear programming problem so the classical techniques break down. Instead of using iterative numerical techniques, we solve these problems using closed-form algebraic expressions. Then, we present several new case studies of optimal analog and digital IIR filters that cannot be designed with classical techniques, and the formal, mathematical framework that underlies their solutions.

2. Design space

We focus our attention on a lowpass prototype filter that serves as the basis for the design of a lowpass, highpass, bandpass, or bandstop filter. First, we map the user specification into a characteristic function specification S_K to provide a clearer relationship between the design parameters and the specification

$$S_K = \{F_p, F_s, K_p, K_s\} \tag{1}$$

Next, we identify the design parameters. Finally, we calculate the limits of the design parameters. The symbols F_p and F_s designate the passband edge frequency and the stopband edge frequency, respectively, in Hz.

An infinite number of characteristic functions that fit S_K exist. We consider the *elliptic function approximation*, because it fulfills the requirements with the minimal transfer function order. The minimal order can often lead to the most economical solution (the minimal number of components, the minimal number of multiplications, and so forth).

The *prototype elliptic approximation*, K_e, is an nth-order rational function in the real variable x

$$K_e(x) = \epsilon |R(n, \xi, x)| \tag{2}$$

where R, referred to as the *rational elliptic function*, satisfies the conditions

$$\begin{array}{rcll} 0 & \leq & |R(n,\xi,x)| \leq 1, & |x| \leq 1 \\ L(n,\xi) & \leq & |R(n,\xi,x)|, & |x| \geq \xi \end{array} \tag{3}$$

where L is the minimal value of the magnitude of R for $|x| \geq \xi$

$$L(n,\xi) = |R(n,\xi,\xi)| \tag{4}$$

The normalized transition band $1 < x < \xi$ is defined by

$$1 < |R(n,\xi,x)| < L(n,\xi), \qquad 1 < |x| < \xi \tag{5}$$

The parameter ξ is called the *selectivity factor*.

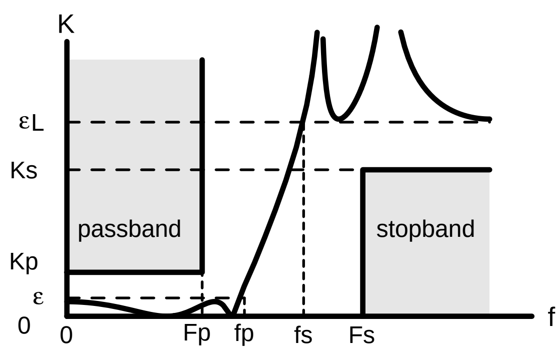

Figure 1. Characteristic function.

The parameter ϵ determines the maximal variation of K_e in the normalized passband $0 \leq x \leq 1$

$$0 \leq K_e(x) \leq \epsilon, \qquad |x| \leq 1 \tag{6}$$

and is called the *ripple factor*.

The *elliptic approximation*, K, is a rational function in frequency ω rad/s, Fig. 1,

$$K(\omega) = K_e(x), \qquad x = \frac{\omega}{2\pi f_p} \tag{7}$$

where f_p represents a design parameter that we call the *actual passband edge*. Traditionally, it has been set to $f_p = F_p$.

The four quantities, n, ξ, ϵ, and f_p, are collectively referred to as *design parameters* and can be expressed as a list of the form

$$D = \{n, \xi, \epsilon, f_p\} \tag{8}$$

Each of the listed parameters can take a value from a continuous range (ξ,ϵ,f_p) or discrete range (n) of numbers. The order n is also referred to as the *filter order*. The ordinary elliptic function provides the minimal order, $n_{min} = n_{ellip}$, for a given specification. The maximal order, from the practical viewpoint, can be assumed to be $n_{max} = 2\,n_{min}$.

The selectivity factor, ξ, ripple factor ϵ and actual passband edge f_p fall within the limits which are found in [7]. The set of all quadruples $D = \{n, \xi, \epsilon, f_p\}$, satisfying the constraints $\{n_{min} \leq n \leq n_{max}$, $\xi_{min} \leq \xi \leq \xi_{max}$ and $\epsilon_{min} \leq \epsilon \leq \epsilon_{max}$, $f_{p,min} \leq f_p \leq f_{p,max}\}$ is called the *design space*.

$$D_S = \{D_{S,n}\}_{n=n_{min}, n_{min}+1, \ldots, n_{max}} \tag{9}$$

$$D_{S,n} = \left\{ \begin{array}{ccccc} & & n & & \\ \xi_{min}(n) & \leq & \xi & \leq & \xi_{max}(n) \\ \epsilon_{min}(n,\xi) & \leq & \epsilon & \leq & K_p \\ f_{p,min}(n) & \leq & f_p & \leq & f_{p,max}(n)\} \end{array} \right. \tag{10}$$

Since the integer order n takes only discrete numeric values, it is more convenient to express the design space, D_S, as a list of subspaces, $D_{S,n}$:

$$\left\{ \begin{array}{l} \left\{ \begin{array}{ccccc} & & n = n_{min} & & \\ \xi_{min}(n) & \leq & \xi & \leq & \xi_{max}(n) \\ \epsilon_{min}(n,\xi) & \leq & \epsilon & \leq & K_p \\ f_{p,min}(n) & \leq & f_p & \leq & f_{p,max}(n) \end{array} \right. \\ \ldots \\ \left\{ \begin{array}{ccccc} & & n = n_{max} & & \\ \xi_{min}(n) & \leq & \xi & \leq & \xi_{max}(n) \\ \epsilon_{min}(n,\xi) & \leq & \epsilon & \leq & K_p \\ f_{p,min}(n) & \leq & f_p & \leq & f_{p,max}(n) \end{array} \right. \end{array} \right. \tag{11}$$

where

$$\begin{array}{ccccc} 0 & < & \epsilon_{min}(n+1) & < & \epsilon_{min}(n) \\ 1 & < & \xi_{min}(n+1) & < & \xi_{min}(n) \\ \xi_{max}(n) & < & \xi_{max}(n+1) & \leq & \infty \\ 0 & \leq & f_{p,min}(n+1) & < & f_{p,min}(n) \\ f_{p,max}(n) & < & f_{p,max}(n+1) & \leq & \infty \end{array} \tag{12}$$

3. Basic design alternatives

This section presents our case studies of a comprehensive set of design alternatives based on the design space.

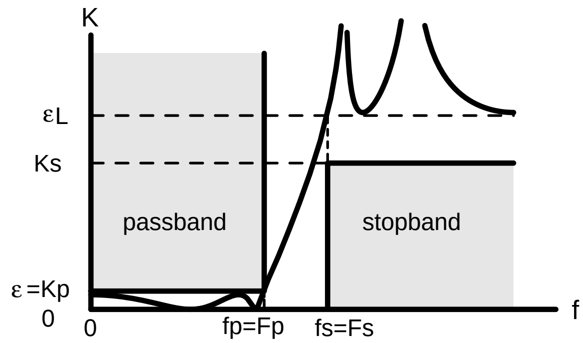

Figure 2. Design D1.

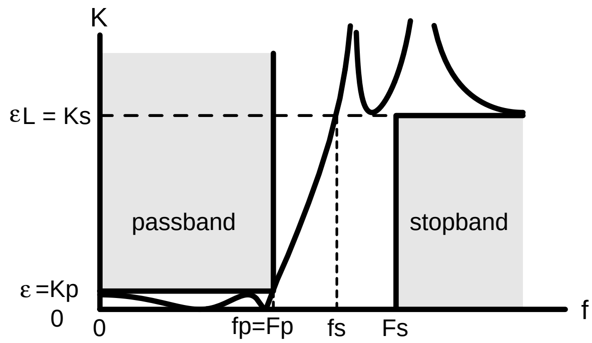

Figure 4. Design D3a.

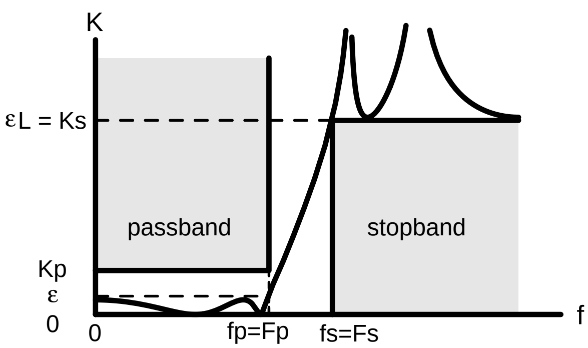

Figure 3. Design D2.

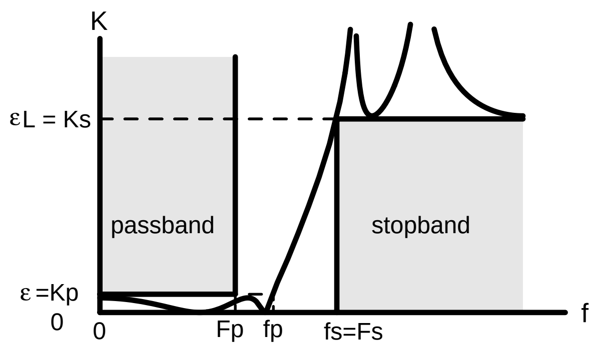

Figure 5. Design D3b.

Design D1 sets the three design parameters, $\xi = F_s/F_p$, $\epsilon = K_p$, $f_p = F_p$, directly from the specification, Fig. 2.

Design D2 sets the two design parameters, $\xi = F_s/F_p$, $f_p = F_p$, directly from the specification, Fig. 3. The ripple factor is computed from $\epsilon = K_s/L(n,\xi)$.

In design D3a, we choose the minimal selectivity factor, $\xi = \xi_{min}$, and set the two design parameters, $\epsilon = K_p$, $f_p = F_p$, directly from the specification, Fig.4.

For design D3b we choose the minimal selectivity factor, $\xi = \xi_{min}$, the same as in the Design 3a, and set the ripple factor, $\epsilon = K_p$, directly from the specification, Fig. 5. The actual passband edge is computed from $f_p = f_{p,max} = F_s/\xi$.

In design D4a we choose the maximal selectivity factor, $\xi = \xi_{max}$, and set the two design parameters, $\epsilon = K_p$, $f_p = F_p$, directly from the specification, Fig.6.

For design D4b we choose the maximal selectivity factor, $\xi = \xi_{max}$, the same as in design D4a, Fig. 7, and calculate the ripple factor from $\epsilon = K_s/L(n,\xi)$. The actual passband edge is computed from $f_p = f_{p,min} = F_s/\xi$.

By increasing the filter order, $n > n_{ellip}$, we arrive at the Chebyshev type approximation, for $n = n_C$; design D4a degenerates from rational polynomial to a polynomial (allpole) filter ($f_p = F_p$, $f_s \to \infty$). Alternatively, for the same order, $n = n_C$, design D4b yields an Inverse Chebyshev type filter ($f_s = F_s$, $f_p \to 0$). When the filter order is equal to the order of the Butterworth type filter, the maximal transition design D4 transforms into an allpole Butterworth type filter ($f_p \to 0$, $f_s \to \infty$). This means that the classical filter types, Chebyshev, Inverse Chebyshev and Butterworth, are just special cases of the elliptic function filters, and are contained within the design space D_S.

4. Example

A lowpass filter will be designed to meet the attenuation specification

$$S_A = \{F_p, F_s, A_p, A_s\} = \{3\text{ kHz}, 3225\text{ Hz}, 0.2\text{dB}, 40\text{dB}\}$$

We will consider the mapped specification

$$S_K = \{F_p, F_s, K_p, K_s\} = \{3\text{ kHz}, 3225\text{ Hz}, 0.2171, 100\}$$

and the actual specification of a realized filter, $S_e = \{f_p, f_s, \epsilon, \epsilon L\}$, where the set of inequalities $\{f_p <$

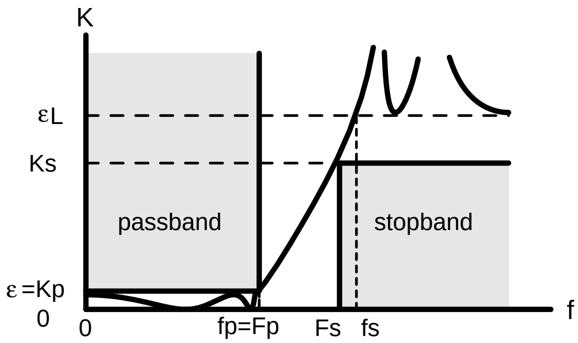

Figure 6. Design D4a.

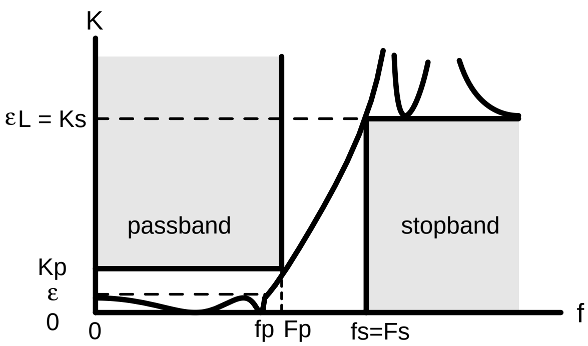

Figure 7. Design D4b.

$F_s, f_s > F_p, \epsilon < K_p, \epsilon L > K_s\}$ must be satisfied. First, the minimal filter order is calculated to be $n = 8$. Next, the range of f_p, f_s and ϵ is determined for $n \geq 8$:

		Filter Order, n			
	Units	8	9	10	$2 \times 6 = 12$
ϵ_{min}	–	0.0910	0.0319	0.0112	0.1044
ϵ_{max}	–	0.2171	0.2171	0.2171	0.2171
$f_{p,max}$	Hz	3092	3156	3189	3101
$f_{s,min}$	Hz	3129	3066	3034	3120
$f_{s,max}$	Hz	3250	3294	3360	3263
Q_{min}	–	24	26	28	15
Q_{max}	–	42	81	156	26

The design subspaces for $n = 8$, $n = 9$ and $n = 13$ are shown in Figs. 8, 9 and 10.

The table shows that the quality factor Q varies from 15 to 156. Some standard programs (like MATLAB) will result in $Q = 42$, which is too high for practical implementations. Classical approximations will be also unacceptable: the order of the Butterworth filter is extremely high ($n = 85$), while the order of the Chebyshev and Inverse Chebyshev type is also high ($n = 18$) with high Q-factors ($Q_{cheb} = 46$ and $Q_{invcheb} = 20$).

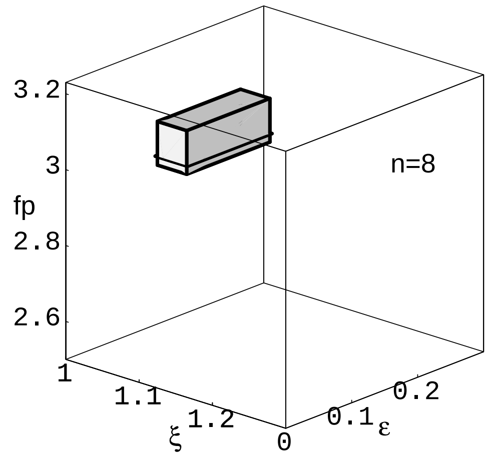

Figure 8. Design space for n = 8.

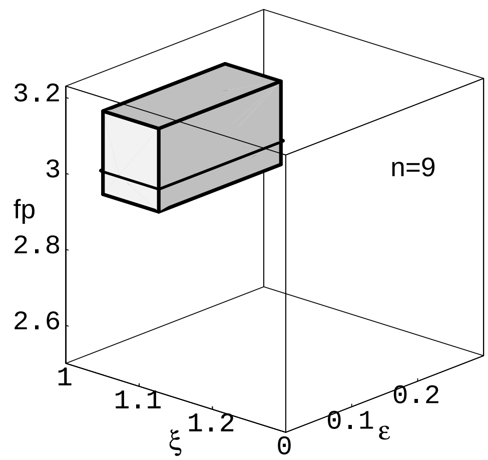

Figure 9. Design space for n = 9.

For the realization of an 8th-order filter, a high-Q building block (with two amplifiers per second-order section) is recommended in [8], and $4 \times 2 = 8$ amplifiers are required. In the case of the 12th-order filter, medium-Q building blocks are preferred (with 1 amplifier per second-order section), hence 6 amplifiers are used. Therefore, in spite of the increased filter order, two fewer amplifiers are used, the power dissipation is lower, and better dynamic range and smaller group delay variation are obtained.

The range of ξ, ϵ, f_p and f_s are shown in Figs. 11 and 12. The minimal filter order, $n = n_{min}$ implies a small range for the design parameters and the optimization of filter behavior can be ineffective.

It is also worth noticing that increasing the filter order, $n > n_{min}$, does not necessarily lead to a better solution; however, in many practical filter designs, the improvement was considerable. For example, the clas-

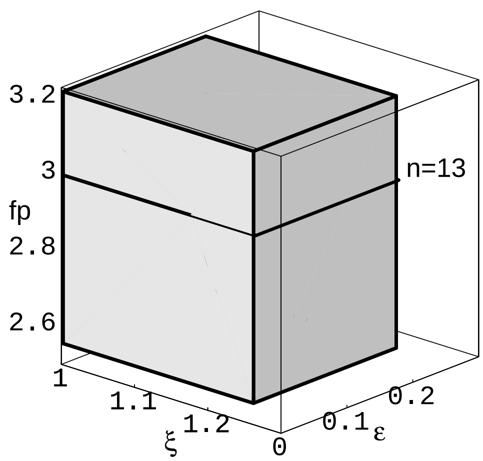

Figure 10. Design space for n = 13.

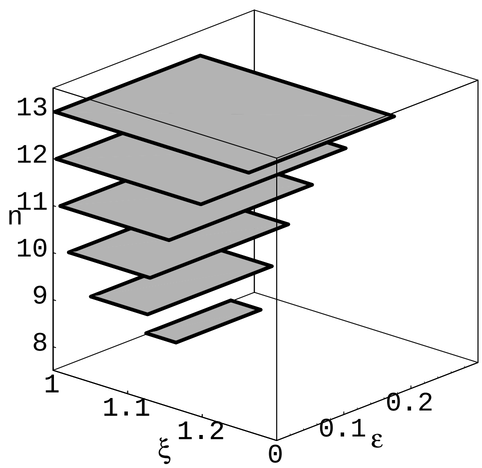

Figure 11. Design space of ξ, ϵ and n.

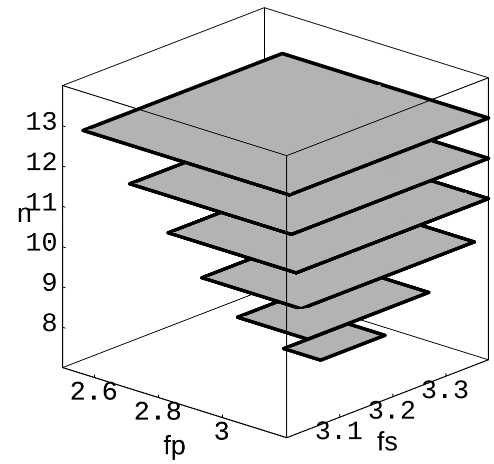

Figure 12. Design space of f_p, f_s and n.

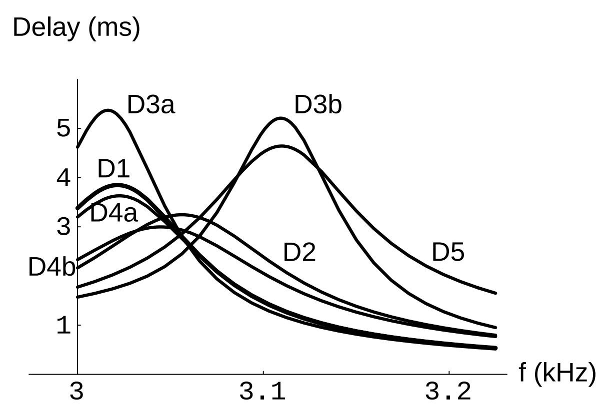

Figure 13. Delay in the transition region.

sical filter design failed to meet the specification in the case of a switched capacitor (SC) filter. However, a design based on our approach was implemented, and the measured filter characteristics showed that advanced filter design was successful [5]. The group delay of the basic designs are plotted in Figs. 13 and 14.

The maximum delay is obtained for minimal transition designs, D3a and D3b, while the maximal transition designs, D4a and D4b, have lower group delay variation. Design D3b has the minimal variation of the group delay in the passband, while the similar design D3a has the highest overall group delay variation. Design D5, which is based on the minimal Q-factor prototype [2], also has a small variation of group delay in the passband.

The step responses of the basic designs are shown in Fig. 15. The shape of all responses is the same with approximately the same amount of overshoots (D3a and D3b have the largest overshoot). As we expect, D4b has the smallest time delay. However, design D4a, which also has good group delay characteristics, has the worst time delay.

Finally, we present the attenuation characteristic of a multiplierless IIR digital filter, which was designed by using the proposed advanced design technique, shown in Fig. 16. For the minimal filter order, $n = 7$, it was impossible to design a multiplierless filter, because coefficient quantization makes the design fail to meet the specification $S_A = \{F_p, F_s, A_p, A_s\} = \{3.4 \text{ kHz}, 4.3 \text{ kHz}, 0.2 \text{ dB}, 65 \text{ dB}\}$, $F_{samp} = 16$ kHz. By increasing the filter order from 7 to 9, we enlarge the design space. Next, we find the closed-form expressions for all coefficients in terms of the selectivity factor ξ (design D5 was selected). Then, we optimize ξ by minimizing the error function constructed as a sum of squared differences between calculated coefficient values and power-of-two values.

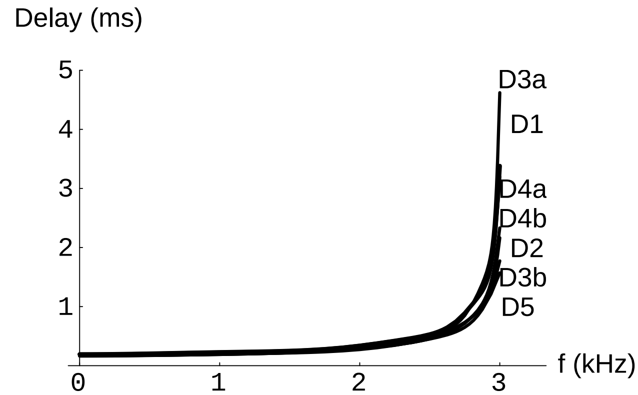

Figure 14. Delay in the passband.

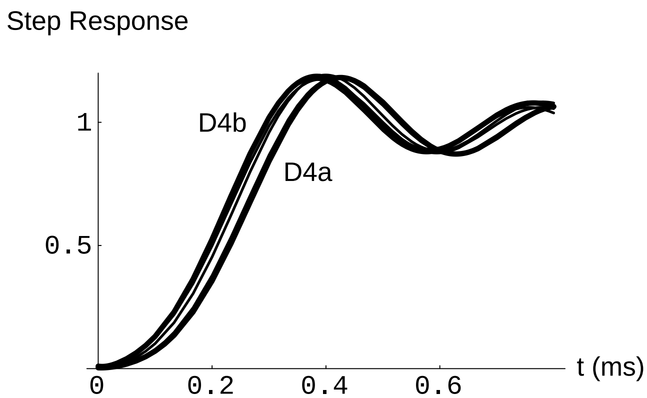

Figure 15. Step responses of basic designs.

5. Conclusion

We present several case studies of optimal analog and digital IIR filter design, and show that conventional approaches to filter design either return only one design thereby hiding a wealth of robust alternatives or fail to find a design when a design exists. We develop advanced design techniques to find a comprehensive set of optimal designs to represent the infinite solution space. The optimal designs include filters that have minimal order, minimal quality factors, minimal complexity, minimal number of multipliers, power-of-two multipliers, etc. We have observed that many designs satisfy the same user specification, and that minimum-order filters may not be as efficient to implement as some higher-order filters.

References

[1] D. Rabrenović and M. Lutovac. Minimum stopband attenuation of the Cauer filters without el-

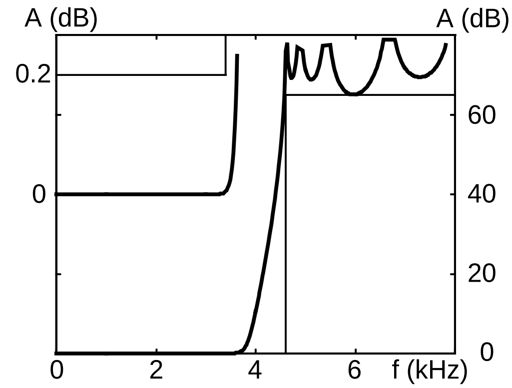

Figure 16. Attenuation of multiplierless digital IIR filter with coefficients: α_1**=** -$1/2^5$, α**=** -$1/2^4$, β_2**=** $1/2^2 + 1/2^4$ - $1/2^6$, β_3**=** 1 - $1/2^3$ - $1/2^5$ - $1/2^9$ $+ 1/2^{12}$, β_4**=** $1/2^3$ - $1/2^5$ - $1/2^7$ - $1/2^{10}$, β_5**=** $1/2 + 1/2^4$ - $1/2^9$, $\xi = 1.766$.

liptic functions and integrals. *IEEE Trans. Circ. Systems - Part I*, CAS-40: 618–621, Sep. 1993.

[2] D. Rabrenović and M. Lutovac. Elliptic filters with minimal Q-factors. *Electronics Letters*, 30(3): 206-207, Feb. 1994.

[3] S. Wolfram. *Mathematica: A System for Doing Mathematics by Computer*. Addison-Wesley, 1991.

[4] M. D. Lutovac, D. Tošić, and B. Evans. Algorithm for symbolic design of elliptic filters. *Proc. Symbolic Methods Analog Circuit Design*, Leuven, Belgium, Oct. 1996.

[5] M. D. Lutovac, D. Novaković, and I. Markoski, Selective SC-filters with low passive sensitivity. *IEE Electronics Letters*, 33(8): 674-675, 1997.

[6] L. Milić and M. D. Lutovac. Reducing the number of multipliers in the parallel realization of half-band elliptic IIR filters. *IEEE Trans. Signal Processing*, 44(10), 2619-2623, Oct. 1996.

[7] M. D. Lutovac, D. V. Tošić, B. L. Evans. Design space approach to advanced filter design. *Proc. Telsiks'97*, Niš, Yugoslavia, Oct. 1997. (invited paper).

[8] G. Moschytz and P. Horn. *Active Filter Design Handbook*. John Wiley, Chichester, 1981.